Cannabinoid Type 1 Receptors are Upregulated during Acute Activation of Brown Adipose Tissue

Minna Lahesmaa[1,2], Olof Eriksson[3,4], Thorsten Gnad[5], Vesa Oikonen[1], Marco Bucci[1], Jussi Hirvonen[1,6], Kalle Koskensalo[1,2], Jarmo Teuho[2], Tarja Niemi[7], Markku Taittonen[8], Salla Lahdenpohja[1], Mueez U Din[1], Merja Haaparanta-Solin[1,9], Alexander Pfeifer[5], Kirsi A. Virtanen[1,2], Pirjo Nuutila[1,10]

1. Turku PET Centre, University of Turku, Turku, 20520, Finland
2. Turku PET Centre, Turku University Hospital, Turku, 20520, Finland
3. Turku PET Centre, Åbo Akademi, Turku, 20520, Finland
4. Department of Medicinal Chemistry, Uppsala University, Uppsala, 751 83 Sweden
5. Institute of Pharmacology and Toxicology, University of Bonn, Bonn, 53105, Germany
6. Department of Radiology, University of Turku, Turku, 20520, Finland
7. Department of Plastic and General Surgery, Turku University Hospital, Turku, 20520, Finland
8. Department of Anesthesiology, Turku University Hospital, Turku, 20520, Finland
9. MediCity Research Laboratories, University of Turku, Turku, 20520, Finland
10. Department of Endocrinology, Turku University Hospital, Turku, 20520, Finland

Corresponding Author:

Prof. Pirjo Nuutila, M.D., PhD
e-mail: pirjo.nuutila@utu.fi
telephone: +35840 162 6834
Turku PET Centre
University of Turku
P.O. Box 52, FI-20520, Turku, Finland

Word count: 4213
Tables: 2
Figures: 3

Key words: Brown adipose tissue; Endocannabinoid; Metabolism; Human; Positron Emisson Tomography (PET); Overweight; Rimonabant

Abstract

Activating brown adipose tissue (BAT) could provide a potential approach for the treatment of obesity and metabolic disease in humans. Obesity is associated with up-regulation of the endocannabinoid system, and blocking the cannabinoid type 1 receptor (CB1R) has been shown to cause weight loss and decrease cardiometabolic risk factors. These effects may partly be mediated via increased BAT metabolism, since there is evidence that CB1R antagonism activates BAT in rodents. To investigate the significance of CB1R in BAT function, we quantified the density of CB1R in human and rodent BAT using the positron emission tomography (PET) radioligand [^{18}F]FMPEP-d_2, and in parallel measured BAT activation with the glucose analogue [^{18}F]FDG. Activation by cold exposure markedly increased CB1R density ~~expression~~ and glucose uptake in BAT of lean men. Similarly, β3-receptor agonism increased CB1R density ~~expression~~ in BAT of rats. In contrast, overweight men with reduced BAT activity exhibited decreased CB1R in BAT, reflecting impaired endocannabinoid regulation. Image-guided biopsies confirmed CB1R mRNA expression in human BAT. Furthermore, CB1R blockade increased glucose uptake and lipolysis of brown adipocytes. Our results highlight that CB1Rs are significant for human BAT activity, and the CB1R provide a novel therapeutic target for BAT activation in humans.

Clinical Trials Identifier NCT02941172

Brown adipose tissue (BAT) has emerged as a potential target to combat obesity and metabolic disease in humans. Activation of BAT is beneficial for human metabolism at a systemic level, because it increases metabolic rate [1] and is associated with increased lipid and glucose disposal [2–5]. BAT can be activated by stimulating the sympathetic nervous system with cold exposure or β3-adrenergic receptor (β3-AR) agonists [1,6,7]. However, BAT function is also controlled by a number of other factors [8–10], which currently are poorly understood and largely unexplored.

The endocannabinoid system (ECS) and specifically the cannabinoid type 1 receptors (CB1R) control lipid and glucose metabolism [11]. The ECS consists of a network of receptors, their endogenous lipid ligands, and enzymes, which are significant in the brain and many peripheral tissues for modulating complex processes including metabolism. Activation of CB1R promotes conservation of energy by increasing food intake and inhibiting energy expenditure and thermogenesis, leading to fat mass expansion [12]. Conversely, blockade of CB1R has been found to decrease body weight and fat mass, improve glucose homeostasis and insulin sensitivity, and decrease cardiometabolic risk factors, making CB1R antagonists potential drugs against obesity and diabetes [13]. CB1R antagonist rimonabant (SR141716) was previously in clinical use with strong efficacy for weight loss, but was withdrawn due to serious psychiatric adverse effects [14]. Recently, novel CB1R antagonists which act strictly peripherally have been found to activate BAT in rodents, inducing lipolysis and lipid oxidation, thus improving metabolism [15,16]. Activation of BAT via CB1R antagonism without harmful centrally mediated adverse effects could be one way to improve metabolic disease and combat obesity in humans [17].

CB1R physiology and pathology can be studied *in vivo* using positron emission tomography (PET). The CB1R radioligand [^{18}F]FMPEP-d_2 has previously been used to quantify the density of CB1R in the human brain [18–20]. So far, this radioligand has not been used to study CB1R of other tissues in humans. Recently, we have shown in rodents that [^{18}F]FMPEP-d_2 binds to BAT *in vivo*, indicating high CB1R density in BAT [21]. There is also preclinical evidence that CB1R and endocannabinoids are upregulated in BAT following cold or β3-AR activation [22]. Here we designed a clinical study aiming to investigate CB1R density in human brown fat using [^{18}F]FMPEP-d_2-PET imaging in baseline and cold conditions. We also evaluated the effect of obesity

on CB1R density in BAT and other tissues including the brain. We found that CB1 receptors ~~expression~~ are up-regulated when BAT is metabolically activated by cold, but this response is blunted in overweight subjects. CB1R mRNA expression in human BAT was confirmed from image-guided biopsies. In pre-clinical pharmacological experiments, CB1R antagonism was shown to increase glucose uptake and lipolysis of brown adipocytes.

RESEARCH DESIGN AND METHODS

Human studies

Study subjects

The clinical PET study included 18 healthy males, who were divided to a lean group (n=9) and an overweight group (n=9), based on the combination of BMI (lean < 25 kg/m^2), waist circumference (lean < 100cm) and body fat percentage (lean <20%). The subjects were all Caucasian men, with an average age of 33 years (range 21-54 years). Subjects were determined healthy by means of clinical examination, blood tests and anthropometric measurements. (See Tables 1 and 2). The study protocol was reviewed and approved by the Ethics committee of the Hospital District of Southwest Finland and was conducted according to the principles of the Declaration of Helsinki. All study subjects provided written informed consent.

Study design

Each subject was studied on three separate days after an overnight fast of 8-10 hours (Figure 1A-1D). To measure CB1R density, dynamic positron emission tomography/computed tomography (PET/CT) examinations were performed using the CB1R inverse agonist radioligand [^{18}F]FMPEP-d_2, once in room temperature conditions (RT) and once during controlled cold exposure. To determine whether the subject had metabolically active BAT, a PET/magnetic resonance (PET/MR) study using the glucose analogue [^{18}F]FDG was performed during controlled cold exposure. The radioligands [^{18}F]FMPEP-d_2 and [^{18}F]FDG were

synthesized according to standard operating procedures of the Turku PET Centre as previously described [23,24].

[^{18}F]FDG PET/MR scanning protocol and image analysis

Glucose uptake of BAT in the neck area was measured during cold exposure after a standardized 2-hour cooling protocol with cooling blankets [25] (see Supplemental Material). 148 ± 13 MBq of [^{18}F]FDG was injected i.v. and a 40 min dynamic PET scan of the cervical region was performed using a 3T Philips Ingenuity TF PET/MR scanner (Philips Health Care, Amsterdam, Netherlands). Eight consecutive modified 2-point Dixon sequences (mDixon) were used to provide anatomical reference in the whole body area and for calculating signal fat fraction (SFF) maps (see Supplemental Material). Image analysis was performed using Carimas 2.9 software (Turku PET Centre, Turku, Finland). BAT regions of interest (ROI) were identified in supraclavicular depots of adipose tissue, confirmed with MR SFF maps, and glucose uptake was quantified using the Patlak linearization model [26].

[^{18}F]FMPEP-d_2 PET/CT scanning protocol and image analysis

To measure CB1R density in different tissues, areas of the neck, abdomen and brain were scanned using a PET/CT scanner (GE Discovery STE[16]**,** General Electric Medical Systems, Milwaukee, WI, U.S.A.) once in RT and once during standardized cold exposure. 152 ± 12 MBq of [^{18}F]FMPEP-d_2 was injected i.v. and dynamic scans of the cervical region (60 min), abdominal area (9 min) and the brain (9 min) were conducted. CT scans were performed of each region for photon attenuation and anatomical reference.

Carimas 2.9 software was used for image analysis of BAT, WAT and muscle. ROIs of adipose tissue were manually drawn on the fused PET/CT images, including only voxels with CT Hounsfield units (HU) within the adipose tissue range (-50 - -250 HU) [27]. BAT ROIs were drawn bilaterally in supraclavicular adipose tissue depots, subcutaneous and intraperitoneal WAT ROIs in abdominal regions, and muscle ROIs in the

trapezius muscle. Regional time-activity-curves (TAC) were calculated from the dynamic images. Details about data acquisition, PET image analysis, determination of plasma input, metabolite corrections, modeling of the data and brain image analysis (using SPM12 software) are available in the Supplemental Material. CB1R density of a tissue can be determined by calculating the volume distribution (V_T) or fractional uptake rate (FUR) of [^{18}F]FMPEP-d_2 from the dynamic PET images. Briefly, volume distribution (V_T) was calculated from the supraclavicular BAT regions by applying the reversible one-tissue compartmental model, using the metabolite corrected plasma TAC as model input [21]. Fractional uptake rate (FUR) was also calculated for BAT, WAT, muscle, and brain, in order to quantitatively compare CB1R density between the tissues.

Animal studies

Sprague Dawley rats (n=39, male, 8-10 weeks old, 228 ± 28g) were bred at the animal facility of the University of Turku. All animal experiments were approved by the Regional State Administrative Agency for Southern Finland (ESAVI/3899/04.10.07/2013), and animal care complied with the principles of laboratory animal care and with guidelines of the International Council of Laboratory Animal Science (ICLAS). The animals were housed at 21±3°C, in an atmosphere of humidity 55±15 %, with a light period from 6.00 a.m. to 6.00 p.m. All animals had free access to RM1 (E) chow (801002; Special Diets Service, Witham, UK) and tap water.

Pretreatment of animals prior to PET scanning

The rats were divided into three groups (n=13), each being administered radioligand alone or radioligand following 10 min i.v. pre-administration 2 mg/kg of β3-AR agonist CL 316243 (Sigma) or 2 mg/kg of CB1R antagonist rimonabant (Sigma). Briefly, CL 316243 was dissolved in 0.9% NaCl prior to injection. Rimonabant was dissolved in EtOH (150 µl), and then diluted in biocompatible polar solvent Kleptose (β-cyclodextrin, Apoteket, Uppsala University Hospital, Uppsala, Sweden) to a final EtOH concentration of 20% before injection.

[^{18}F]FMPEP-d_2 and [^{18}F]FDG PET scanning procedures and image analysis

Detailed imaging procedures, data acquisition and analysis are described in the Supplemental Material. Briefly, each rat was sedated, and anesthesia was maintained throughout the imaging studies. Animals were positioned in the PET/CT scanner with the BAT in the center of the field of view. 9.7 ± 2.0 MBq of [^{18}F]FMPEP-d_2 (corresponding in all cases to <0.1µg/kg) was administered i.v. in the tail vein (n=24, or n=8 from each treatment group). Each rat was then examined by PET/CT over 120 min. V_T of [^{18}F]FMPEP-d_2 in BAT in each rat was calculated in the PMOD kinetic modeling module (PKIN, PMOD technologies, Zurich, Switzerland) using the one-tissue compartment model as previously described [21].

20.1 ± 1.6 MBq of [^{18}F]FDG was administered i.v. in the tail vein in another group of rats (n=15, or n=5 from each treatment group). Each animal was then examined by PET/CT over 60 min. The glucose utilization (in µmol/100g/min) in BAT was estimated by fitting the PET data to a [^{18}F]FDG two-tissue compartment model, using a lumped constant of 1.3.

Ex vivo organ distribution studies

After the PET scanning the animals were sacrificed (120 min post [^{18}F]FMPEP-d_2 injection (n=24) or 60 min post [^{18}F]FDG injection (n=15)). Tissues were excised and measured in an automatic γ-counter (Wizard^2, PerkinElmer, Finland). Measured radioactivity was corrected for decay, weight of the organ, and background, and it was expressed as percentage of the injected dose/gram of tissue (%ID/g).

***In vitro* studies**

Human BAT biopsies

Nine out of the eighteen subjects who underwent PET imaging gave additional written consent for acquiring BAT biopsies from the supraclavicular neck region (5 lean subjects, 4 overweight subjects). In sterile, operating room conditions with an anesthesiologist monitoring the procedure, biopsies of BAT were taken by a plastic surgeon through one small skin incision, using local anesthesia. Anatomical location of BAT was

pre-determined with [^{18}F]FDG PET/MR images. After removal, samples were immediately snap-frozen into liquid nitrogen and stored in -70°C until analysis.

Human cells

Human multipotent adipose-derived stem cells (hMADS) were obtained from C. Dani and differentiated into brown adipocytes as described [28]. Human white adipocytes were obtained from PromoCell and differentiated according to manufacturer's instructions.

Cannabinoid receptor expression analysis

Total RNA was isolated using Trizol (human cells) or NucleoSpin RNA XS (Machery-Nagel; human BAT samples). cDNA synthesis was performed with ProtoScript First Strand cDNA Synthesis Kit (NEB) according to manufacturer's instructions. Human cannabinoid receptor mRNA expression was analyzed using a ABI 7900HT fast real time PCR machine with SybrGreen (Roche) and expression was calculated as 2^-dCt relative to TATA-box binding protein, TBP. PCR details are described in the Supplemental Material. mRNA of CB1R was measured at baseline and after incubation with 1 µM noradrenaline for 16 h.

Lipolysis and glucose uptake assays

To measure lipolysis, differentiated hMADS were washed twice with lipolysis medium (Life Technologies, DMEM21603) supplemented with 2% w/v fatty acid–free BSA (Sigma-Aldrich) followed by incubation with lipolysis medium containing 100 nM of each antagonist/inverse agonist (CB1: SR141716A; CB2: SR144528), each agonist (CB1: ACEA; CB2: JWH133), and/or 1 µM NA at 37°C and 5% CO_2 for four hours. Antagonists were added 20 minutes prior to NA treatment. All substances were purchased from Tocris. 50 µl cell culture media was collected per well and incubated with 50 µl Free Glycerol Reagent (Sigma-Aldrich) for 5 min at 37°C. Absorption was measured at 540 nm. Glycerol release was calculated with glycerol standard (Sigma-Aldrich) and normalized to protein content. To measure glucose uptake, hMADS were differentiated in 12

well plates, starved for 16 h, treated with indicated substances (see above) for 20 min and glucose uptake assay (Abcam #136955) was performed according to manufacturer's instructions. Antagonists were added 20 minutes prior to NA treatment. Experiments were performed with four independent cell cultures.

Statistical methods

Results are presented as means ± standard deviations (S.D.). Paired two-tailed student t-test (α=0.95) was used for assessing differences between baseline and cold conditions within a group, whereas unpaired two-tailed student t-test (α=0.95) was used for assessing differences between lean and overweight groups. Similarly the unpaired two-tailed student t-test (α=0.95) was used for assessing differences between treatment groups of rats and for cell experiments. Pearson's correlations were used to study associations between [^{18}F]FMPEP-d_2 FUR in human brain and BAT, BAT glucose uptake and UCP-1 expression. Statistical analyses were performed using IBM SPSS 23.0 software.

RESULTS

Cold increases CB1 receptor density in supraclavicular BAT of lean and overweight men

Compared to baseline conditions, acute cold exposure increased fractional uptake rate (FUR) of the CB1R radioligand in supraclavicular BAT by 3-fold in lean subjects (P=0.006, Figure 1E), indicating higher CB1R density. Interestingly, overweight subjects exhibited low CB1R density at baseline, which increased during cold exposure (P=0.026, Figure 1E), but only reached the baseline levels of lean subjects. Importantly, the uptake of [^{18}F]FMPEP-d_2 in BAT correlated strongly with the degree of functional BAT activity, as measured by its glucose uptake in cold (R=0.89, P<0.001) (Figure 1F). Additionally, cold markedly increased energy expenditure in both lean and overweight subjects (Table 2). Volume distribution (V_T) and fractional uptake rate (FUR) of [^{18}F]FMPEP-d_2 are both indices of CB1R density in tissue. BAT V_T correlated with BAT FUR in room temperature (R=0.80, P<0.001) and cold conditions (R=0.73, P=0.001), hence FUR is a suitable index for CB1R density when V_T is unavailable. (For details see Supplemental Material.)

CB1 receptors are expressed in human BAT

To verify our imaging findings, we analyzed image-guided BAT biopsies from 9 study subjects, specifically studying BAT markers (uncoupling protein-1 (UCP-1), β3-adrenergic receptors) and the type 1 (CB1) and type 2 (CB2) cannabinoid receptors. We found that mRNA expression of CB1R was higher compared to that of CB2R (P=0.039), but no significant difference was found between lean and overweight subjects (Figure 1G). mRNA expression of UCP-1 was significantly higher in lean than overweight subjects (P=0.02, Figure 1I). When biopsy data from lean (n=5) and overweight (n=4) subjects were pooled, UCP-1 mRNA expression correlated with BAT [^{18}F]FMPEP-d_2 uptake (R=0.73, P=0.027, Figure 1J) as well as glucose uptake in cold (R=0.76, P=0.028, Figure 1K).

Overweight and cold exposure cause changes in human brain CB1R density

The central nervous system is essential in mediating cannabinoid signaling and BAT activation. When we quantified the CB1R density of the brain in RT, CB1R density was 23% lower in overweight than in lean subjects (Figure 2A-B). Cooling increased CB1R density in the pooled group, (P=0.033), specifically in the areas of the midbrain, pons and parietal lobe. Furthermore, a positive correlation was found between [^{18}F]FMPEP-d_2 uptake in BAT and brain gray matter, in cold conditions (P<0.0005) but not at baseline (midbrain region shown in Figures 2D-E).

Overweight decreases CB1 receptor density in white adipose tissue

In overweight subjects, uptake of [^{18}F]FMPEP-d_2 in WAT both subcutaneously and intraperitoneally was significantly lower compared to lean subjects, while uptake in muscle was similar in both groups (Figure 2A). Interestingly in lean subjects, cold exposure induced a tendency of higher CB1R density in abdominal intraperitoneal fat (P=0.07, Figure 2A).

Pharmacological rodent studies confirmed CB1 receptor specific binding of [^{18}F]FMPEP-d_2

To better understand CB1R physiology and the suitability of this tracer for BAT imaging, we conducted further PET studies in rats during pharmacological activation of BAT and blockade of CB1R. Similarly to humans, [^{18}F]FMPEP-d_2 uptake markedly increased in interscapular BAT following i.v. administration of the β3-AR agonist CL 316243 (Figure 3A). This clear increase persisted also when taking possible alterations of [^{18}F]FMPEP-d_2 metabolism into account by kinetic modeling (Figure 3B). The *in vivo* activation of BAT by CL 316243 was confirmed by increased glucose utilization (Figure 3C), and BAT perfusion (Figure 3D). Pre-administration of the CB1R antagonist rimonabant inhibited the [^{18}F]FMPEP-d_2 uptake in BAT (Figure 3B) and brain at basal conditions ($P<0.0001$), indicating that the uptake was receptor mediated rather than non-specific. However, CB1R antagonism with an i.v. dose of 2 mg/kg did not significantly alter interscapular BAT glucose uptake nor modulate perfusion (Figures 3C, 3D).

Pharmacological characterization of human brown adipocytes

Receptor mRNA expression analyzed in a human brown adipocyte cell line (hMADS) and primary human white adipocytes revealed significantly higher CB1R mRNA expression in brown compared to white adipocytes. Noradrenaline (NA) stimulation significantly increased the mRNA expression of CB1R in brown adipocytes (BA) but significantly decreased it in white adipocytes (WA). No changes were observed in CB2R mRNA expression with NA. (Figures 3E-F).

We further studied the effect of cannabinoid receptor agonism and antagonism on the function of human BA *in vitro*. Pharmacological blockade of CB1R increased glucose uptake, whereas CB1R stimulation, CB2R stimulation and CB2R blockade had no effect (Figure 3G). Activation of human BA with NA increased glucose uptake, and CB1R antagonism further enhanced this increase (Figure 3G). Again, CB1R or CB2R agonism and CB2R antagonism combined with NA had no effect (data not shown). Lipolysis is another

hallmark of BA activation, so we analyzed if CB receptors can modulate glycerol release from human BA. Blocking the CB1R significantly increased lipolysis while CB1R stimulation had no effect (Figure 3H). CB1R blockade after maximal stimulation of BA with NA increased lipolysis, albeit not significantly. Taken together, these data show that CB receptors are expressed in human BA and that CB1R blockade can positively modulate BA function cell autonomously.

DISCUSSION

To our knowledge, this is the first study investigating CB1R expression and function in human BAT *in vivo*. Our imaging results show that acute cold exposure markedly increases [^{18}F]FMPEP-d_2 binding in supraclavicular BAT depots of lean healthy men, indicating increased CB1R density when BAT is activated. CB1R mRNA expression in human BAT was also confirmed from image-guided biopsies. A physiological increase in receptor density suggests that the endocannabinoid system (ECS) plays a role in the activation of human BAT.

Our results are consistent with a previous study in mice showing that stimulation of BAT by cold and β3-AR agonism increased endocannabinoid levels in BAT [22]. Moreover, activation of primary brown adipocytes induced transcription of *Cnr1*, the gene encoding the CB1R [22]. CB1R agonism promotes a positive energy balance [12], hence with their findings Krott et al. hypothesized a negative feedback mechanism, where endocannabinoids, their enzymes and receptors are up-regulated during BAT activation as a potential auto-regulatory loop to inhibit thermogenesis [22]. In line with this, another recent study measured increased plasma endocannabinoid levels of healthy lean men after mild acute cold exposure [29]. This study however did not find correlations between human BAT activity and plasma cannabinoids, as here with our dynamic and highly sensitive PET imaging methods we show a positive association between CB1R density and glucose uptake in human BAT during cold exposure. UCP-1 mRNA expression measured from BAT biopsies was also positively associated with CB1R density and glucose uptake in BAT (n=9, pooled lean and overweight

subjects). An acute cold stress may stimulate the ECS to provide more CB1R for endocannabinoid binding in BAT, in order to inhibit excess energy expenditure and return homeostasis towards a positive energy balance.

Endocannabinoids are produced on demand, acting primarily in the brain, but exerting important regulatory effects on metabolism in adipose tissue [30]. During cold exposure, CB1R were also upregulated in the brain, specifically in the areas of the midbrain, pons and parietal lobe, which are closely related to the sympathetic control of BAT function. Furthermore, CB1R density in the midbrain correlated positively with BAT CB1R density in cold, but not warm conditions. These results indicate a relationship between the ECS, the sympathetic nervous system (SNS) and BAT. The midbrain region includes the hypothalamus, which is one key site for controlling homeostasis and energy expenditure, and where endocannabinoids play a major regulatory role [31]. The parietal lobe receives and processes sensory input, including temperature, while the pons is a significant signaling route controlling autonomic functions [32]. Temperature is sensed in peripheral tissues and information is received and processed in these areas of the central nervous system, after which efferent sympathetic outflow in the form of noradrenaline is increased to BAT, resulting in increased thermogenesis [6]. Endocannabinoid signaling in the brain and in BAT seem to be up-regulated acutely in cold and this may inhibit an excessive thermogenic response [22].

In overweight subjects, CB1R density in BAT was low and the increase in cold was blunted, merely reaching the baseline values of lean subjects, possibly reflecting the generally reduced activity of BAT in overweight subjects. However, CB1R density was also significantly lower in abdominal WAT depots and in the brain as compared to lean subjects. This suggests a broader down-regulation of the CB1R, signifying the impaired regulation of the ECS in overweight subjects, which is in line with previous studies. Excessive activation of the ECS is associated with obesity [12], and a negative association between CB1R density in the brain and body mass index has been reported previously [19,20]. Obese subjects have increased circulating endogenous cannabinoid levels, while mRNA expression of CB1R is lower in the WAT of obese subjects compared to

lean subjects [34,35]. Moreover, higher plasma endocannabinoid levels are related with increased abdominal adiposity and cardiometabolic risk factors [36,37]. The CB1R antagonist rimonabant resulted in weight loss in obese patients [13], demonstrating that blocking the overactive ECS could improve metabolism. These findings exhibit the negative feedback loop of the ECS; chronically high amounts of circulating endocannabinoids in obesity are associated with fewer CB1R in brain and adipose tissue.

In addition to studying the physiological effects of cold on CB1R signaling in human BAT, we conducted pharmacological studies targeting the CB receptors in rodents and in a human brown adipocyte system. ~~There is~~ Previous pre-clinical evidence suggests that CB1R blockade enhances BAT function. In mice, CB1R antagonists blocked the inhibition of β3-AR leading to increased activation in BAT, lipolysis, and uptake of fatty acids from plasma [38]. Moreover, adipocyte specific CB1R deletion results in browning of WAT, the promotion of a thermogenic program and an increase in alternatively activated macrophages, which increase local NA levels [39]. In human BA, we showed that CB1R antagonism increased glucose uptake and lipolysis, but CB1R agonism, CB2R antagonism or CB2R agonism did not have any effect. During increased NA availability we also measured increased CB1R mRNA expression in BA, but not in WA. Our results add to the existing evidence that, CB1R are significant in regulating brown adipocyte function in a SNS-dependent manner.

Interestingly in rats, we did not measure any appreciable increase in glucose utilization in BAT up to 60 minutes following CB1R antagonist administration, which is in disagreement with previous findings [38,40,41]. This discrepancy may be explained by differences in methodology, such as the acute intravenous dose given here. Longer-lasting plasma exposure to the CB1R antagonist might be required for inducing a recordable increase in glucose utilization in BAT in rat. Unfortunately, the effect of CB1R antagonism in humans could not be investigated in this study due to ethical reasons. No CB1R antagonist is currently in clinical use for humans and the subjects in this study already received the maximal acceptable annual radiation

dose considered safe for healthy volunteers. Future studies need to be done to investigate whether peripheral CB1R antagonism with novel compounds could activate BAT in humans.

One limitation of this study is that the data exhibit only short-term changes in the endocannabinoid system and BAT, lacking the long-term effects. When combining our data and others [22,29], it seems that acutely, BAT can produce endocannabinoids and modulate the density of CB1R available for binding them, in order to adapt to changes in sympathetic tone. We speculate that during prolonged cold exposure, *Cnr1* mRNA expression may increase, but some desensitization of ECS signalling may also occur, similarly to long-term changes seen in obesity. Other long-term adaptations such as expansion of BAT volume and activity, and browning of white adipose tissue may also effect the response. Cold acclimation studies in humans or repeated β3-AR stimulation experiments in rodents are required to understand possible chronic changes and adaptations of the ECS and BAT function.

The CB1R PET radioligand [^{18}F]FMPEP-d_2 has previously been used for neuropsychiatric brain studies and its utilization as a surrogate biomarker for BAT was previously reported in rats [21], but the potential of using it to study human BAT physiology has previously been unexplored. Here, in activated BAT of both humans and rats, we observed a strong increase in [^{18}F]FMPEP-d_2 uptake. Binding was blocked by rimonabant, confirming a CB1R mediated mechanism, while non-specific or off-target binding is negligible. In rats, in addition to increased CB1R binding, we estimate that an increase in perfusion occurred based on the increase in glucose extraction rate. Increased perfusion of BAT is a consequence of increased oxidative metabolism [25,42], and while higher perfusion could also result in more radioligand delivery to the target tissue, perfusion alone could not explain the 6-fold increase in [^{18}F]FMPEP-d_2 binding. Furthermore, we observe active retention of the radioligand in BAT throughout the PET scan, in the form of increased volume distribution (V_T, an index of specific binding). Therefore, the current PET data can be explained by transiently increased expression of the CB1 receptor, in response to cold or β3-AR mediated activation in BAT.

In conclusion, acute adrenergic activation of BAT increases CB1R expression in BAT in humans and rodents. This up-regulation may be a negative feedback response of the endocannabinoid system to inhibit excessive energy expenditure and restore homeostasis, and is likely mediated via the central nervous system. In overweight subjects, CB1R density in BAT, WAT and the brain was significantly lower compared to lean subjects, reflecting impairment of the endogenous cannabinoid system in obesity. We conclude that endocannabinoid signaling via the CB1R is significant in the activation and regulation of human BAT, and targeting CB1R could provide a prospective way to treat obesity and metabolism.

Acknowledgments. The authors wish to thank all the study subjects enrolled in this study for their co-operation, and all the technical staff of Turku PET Centre for their assistance.

Author Contributions. M.L. designed the studies, performed clinical imaging experiments, analyzed data, and prepared the manuscript. O.E. designed the studies, obtained funding, conducted the pre-clinical imaging experiments and data analysis, and edited the manuscript. T.G. conducted pre-clinical in vitro studies and data analysis, and edited the manuscript. V.O., M.B., K.K., J.T and M.H-S. processed and analyzed data. J.H. supervised and contributed to image analysis. T.N. and M.T. conducted acquisition of human tissue biopsies. S.L. provided radioligands for imaging experiments. A.P. obtained funding, supervised the studies and edited the manuscript. K.A.V. and P.N. designed the study, obtained funding, supervised the performance of the studies and data analysis, and edited the manuscript. All authors contributed to the critical revision of the manuscript and approved the final version.

Conflict of Interest. The authors have no conflicts of interest or disclosures relevant to this article.

Funding. The study was financially supported by the Academy of Finland (307402, 259926, 265204, 292839 and 269977), the Paulo Foundation, the Instrumentarium Foundation, the Turku University Hospital Research Funds, and the European Union (EU FP7 project 278373; DIABAT). The study was conducted within the Finnish Centre of Excellence in Cardiovascular and Metabolic Diseases supported by the Academy of Finland, University of Turku, Turku University Hospital and Åbo Akademi University. T.G. was supported by DFG grant GN 108/1-1. A.P. was supported by DFG RTG 1873.

Guarantor Statement. P.N. is the guarantor of this work and, as such, had full access to all the data in the study and takes responsibility for the integrity of the data and the accuracy of the data analysis.

Prior Presentation. Parts of this study were presented at the Keystone Symposium on Obesity and Adipose Tissue Biology, Keystone, Colorado, 22-26 January 2017.

REFERENCES

1. Cypess AM, Weiner LS, Roberts-Toler C, Elía EF, Kessler SH, Kahn PA, et al. Activation of human brown adipose tissue by a β3-adrenergic receptor agonist. Cell Metab. 2015;21:33–8.
2. Blondin D, Tingelstad H, Noll C, Frisch F, Phoenix S, Gurin B, et al. Dietary fatty acid metabolism of brown adipose tissue in cold-acclimated men. Nat. Commun. 2017;8:14146.
3. Chondronikola M, Volpi E, Børsheim E, Porter C, Saraf MK, Annamalai P, et al. Brown Adipose Tissue Activation Is Linked to Distinct Systemic Effects on Lipid Metabolism in Humans. Cell Metab. 2016;23:1200–6.
4. Chondronikola M, Volpi E, Børsheim E, Porter C, Annamalai P, Enerbäck S, et al. Brown adipose tissue improves whole-body glucose homeostasis and insulin sensitivity in humans. Diabetes. 2014;63:4089–99.
5. Orava J, Nuutila P, Lidell M, Oikonen V, Noponen T, Viljanen T, et al. Different metabolic responses of human brown adipose tissue to activation by cold and insulin. Cell Metab. 2011;14:272–9.
6. Cannon B, Nedergaard J. Brown Adipose Tissue: Function and Physiological Significance. Physiol. Rev. 2004;84:277–359.
7. Virtanen KA, Lidell ME, Orava J, Heglind M, Westergren R, Niemi T, et al. Functional Brown Adipose Tissue in Healthy Adults. N. Engl. J. Med. 2009;360:1518–25.
8. Kajimura S, Spiegelman BM, Seale P. Brown and Beige Fat: Physiological Roles beyond Heat Generation. Cell Metab. 2015;22:546–59.
9. Loh RKC, Kingwell BA, Carey AL. Human brown adipose tissue as a target for obesity management; beyond cold-induced thermogenesis. Obes. Rev. 2017 Nov;1227–42.
10. Gnad T, Scheibler S, von Kugelgen I, Scheele C, Kilic A, Glode A, et al. Adenosine activates brown adipose tissue and recruits beige adipocytes via A(2A) receptors. Nature. 2014;516:395.
11. Silvestri C, Di Marzo V. The endocannabinoid system in energy homeostasis and the etiopathology of metabolic disorders. Cell Metab. 2013;17:475–90.
12. Mazier W, Saucisse N, Gatta-Cherifi B, Cota D. The Endocannabinoid System: Pivotal Orchestrator of Obesity and Metabolic Disease. Trends Endocrinol. Metab. 2015;26:524–37.
13. Christopoulou FD, Kiortsis DN. An overview of the metabolic effects of rimonabant in randomized controlled trials: potential for other cannabinoid 1 receptor blockers in obesity. J. Clin. Pharm. Ther. 2011;36:10–8.
14. Christensen R, Kristensen PK, Bartels EM, Bliddal H, Astrup A. Efficacy and safety of the weight-loss drug rimonabant: a meta-analysis of randomised trials. Lancet. 2007;370:1706–13.
15. Hsiao WC, Shia KS, Wang YT, Yeh YN, Chang CP, Lin Y, et al. A novel peripheral cannabinoid receptor 1 antagonist, BPR0912, reduces weight independently of food intake and modulates thermogenesis. Diabetes, Obes. Metab. 2015;17:495–504.
16. Takano A, Gulyás B, Varnäs K, Little PB, Noerregaard PK, Jensen NO, et al. Low brain CB1 receptor occupancy by a second generation CB1 receptor antagonist TM38837 in comparison with rimonabant in nonhuman primates: a PET study. Synapse. 2014;68:89–97.
17. Kunos G, Tam J. The case for peripheral CB(1) receptor blockade in the treatment of visceral obesity and its cardiometabolic complications. Br. J. Pharmacol. 2011;163:1423–31.
18. Terry GE, Hirvonen J, Liow J-S, Seneca N, Tauscher JT, Schaus JM, et al. Biodistribution and dosimetry in humans of two inverse agonists to image cannabinoid CB1 receptors using positron emission tomography. Eur. J. Nucl. Med. Mol. Imaging. 2010;37:1499–506.
19. Hirvonen J, Goodwin RS, Li C-T, Terry GE, Zoghbi SS, Morse C, et al. Reversible and regionally selective downregulation of brain cannabinoid CB1 receptors in chronic daily cannabis smokers. Mol. Psychiatry. 2012;17:642–9.
20. Hirvonen J, Zanotti-Fregonara P, Umhau JC, George DT, Rallis-Frutos D, Lyoo CH, et al. Reduced cannabinoid CB1 receptor binding in alcohol dependence measured with positron emission tomography. Mol. Psychiatry. 2013;18:916–21.
21. Eriksson O, Mikkola K, Espes D, Tuominen L, Virtanen K, Forsback S, et al. The Cannabinoid Receptor-1 Is an Imaging Biomarker of Brown Adipose Tissue. J. Nucl. Med. 2015;56:1937–41.
22. Krott LM, Piscitelli F, Heine M, Borrino S, Scheja L, Silvestri C, et al. Endocannabinoid regulation in white and brown adipose tissue following thermogenic activation. J. Lipid Res. 2016;57:464–73.
23. Donohue SR, Krushinski JH, Pike VW, Chernet E, Lee P, Chesterfield AK, et al. Synthesis, Ex Vivo

Evaluation and Radiolabeling of Potent 1,5-Diphenyl-pyrrolidin-2-one Cannabinoid Subtype-1 (CB(1)) Receptor Ligands as Candidates for In Vivo Imaging. J. Med. Chem. 2008;51:5833–42.
24. Hamacher K, Coenen HH, Stöcklin G. Efficient stereospecific synthesis of no-carrier-added 2-[18F]-fluoro-2-deoxy-D-glucose using aminopolyether supported nucleophilic substitution. J Nucl Med. 1986;27:235–8.
25. u Din M, Raiko J, Saari T, Kudomi N, Tolvanen T, Oikonen V, et al. Human brown adipose tissue [15O]O2 PET imaging in the presence and absence of cold stimulus. Eur. J. Nucl. Med. Mol. Imaging. 2016;43:1878–86.
26. Patlak CS, Blasberg RG. Graphical Evaluation of Blood-to-Brain Transfer Constants from Multiple-Time Uptake Data. Generalizations. J. Cereb. Blood Flow Metab. 1985;5:584–90.
27. Din MU, Raiko J, Saari T, Saunavaara V, Kudomi N, Solin O, et al. Human Brown Fat Radiodensity Indicates Underlying Tissue Composition and Systemic Metabolic Health. J. Clin. Endocrinol. Metab. 2017;102:2258–67.
28. Rodriguez AM, Pisani D, Dechesne CA, Turc-Carel C, Kurzenne JY, Wdziekonski B, et al. Transplantation of a multipotent cell population from human adipose tissue induces dystrophin expression in the immunocompetent mdx mouse. J. Exp. Med. 2005;201:1397–405.
29. Kantae V, Nahon KJ, Straat ME, Bakker LEH, Harms AC, van der Stelt M, et al. Endocannabinoid tone is higher in healthy lean South Asian than white Caucasian men. Sci. Rep. 2017;7:7558.
30. Cani PD, Plovier H, Hul M Van, Geurts L, Delzenne NM, Druart C, et al. Endocannabinoids--at the crossroads between the gut microbiota and host metabolism. Nat. Rev. Endocrinol. 2016;12:133–43.
31. Silvestri C, Di Marzo V. The endocannabinoid system in energy homeostasis and the etiopathology of metabolic disorders. Cell Metab. 2013;17:475–90.
32. Jacobson S, Marcus EM. Neuroanatomy for the neuroscientist. Neuroanat. Neurosci. Boston, MA: Springer US; 2008.
33. Dlugos A, Childs E, Stuhr KL, Hillard CJ, de Wit H. Acute Stress Increases Circulating Anandamide and Other N-Acylethanolamines in Healthy Humans. Neuropsychopharmacology. 2012;37:2416–27.
34. Blüher M, Engeli S, Klöting N, Berndt J, Fasshauer M, Bátkai S, et al. Dysregulation of the peripheral and adipose tissue endocannabinoid system in human abdominal obesity. Diabetes. 2006;55:3053–60.
35. Engeli S, Böhnke J, Feldpausch M, Gorzelniak K, Janke J, Bátkai S, et al. Activation of the peripheral endocannabinoid system in human obesity. Diabetes. 2005;54:2838–43.
36. Côté M, Matias I, Lemieux I, Petrosino S, Alméras N, Després J-P, et al. Circulating endocannabinoid levels, abdominal adiposity and related cardiometabolic risk factors in obese men. Int. J. Obes. 2007;31:692–9.
37. Di Marzo V, Côté M, Matias I, Lemieux I, Arsenault BJ, Cartier A, et al. Changes in plasma endocannabinoid levels in viscerally obese men following a 1 year lifestyle modification programme and waist circumference reduction: Associations with changes in metabolic risk factors. Diabetologia. 2009;52:213–7.
38. Boon MR, Kooijman S, van Dam AD, Pelgrom LR, Berbee JFP, Visseren CAR, et al. Peripheral cannabinoid 1 receptor blockade activates brown adipose tissue and diminishes dyslipidemia and obesity. FASEB J. 2014;28:5361–75.
39. Ruiz de Azua I, Mancini G, Srivastava RK, Rey AA, Cardinal P, Tedesco L, et al. Adipocyte cannabinoid receptor CB1 regulates energy homeostasis and alternatively activated macrophages. J. Clin. Invest. American Society for Clinical Investigation; 2017;127:4148–62.
40. Bajzer M, Olivieri M, Haas M, Pfluger P, Magrisso I, Foster M, et al. Cannabinoid receptor 1 (CB1) antagonism enhances glucose utilisation and activates brown adipose tissue in diet-induced obese mice. Diabetologia. 2011;54:3121–31.
41. Verty ANA, Allen AM, Oldfield BJ. The Effects of Rimonabant on Brown Adipose Tissue in Rat: Implications for Energy Expenditure. Obesity. 2009;17:254–61.
42. Muzik O, Mangner T, Leonard W, Kumar A, Janisse J, Granneman J. 15O PET measurement of blood flow and oxygen consumption in cold-activated human brown fat. J. Nucl. Med. 2013;54:523–31.

Table 1. Characteristics of study subjects.

Anthropometric characteristics	Lean	Overweight
Number of participants (males)	9	9
Age (years)	32 ± 9	34 ± 11
Weight (kg)	77.6 ± 8.2	106.5 ± 11.1***
BMI (kg/m^2)	24.9 ± 1.7	32.9 ± 4.6***
Waist circumference (cm)	83.2 ± 7.1	113.6 ± 10.7***
Waist to hip ratio	0.9 ± 0.04	1.0 ± 0.05***
Body fat percentage (%)	19.4 ± 3.2	27.6 ± 3.7***
Blood pressure systolic (mmHg)	125 ± 8	134 ± 15
Blood pressure diastolic (mmHg)	76 ± 11	80 ± 9
Data are mean ± S.D. ***P<0.001, Independent T-Test.		

Table 2. Fasting plasma biochemistry values of study subjects at the screening visit and before and after cold exposure.

		Lean			Overweight		
Fasting Biochemistry	**Normal range**	**Screening**	**Before cooling**	**After cooling**	**Screening**	**Before cooling**	**After cooling**
Glucose (mmol/l)	(4 - 6)	5.0 ± 0.6	5.2 ± 0.5	5.2 ± 0.5	5.5 ± 0.5	5.6 ± 0.4	5.3 ± 0.3
Insulin (mU/l)		6.1 ± 2.4	5.7 ± 1.7	4.2 ± 1.8	12.9 ± 5.8 ##	13.4 ± 9.8	11.3 ± 6.1
Hb-A1c (% (mmol/mol))	(4-6 (20 – 42))	5.0 ± 0.3 (31.1 ± 3.0)			5.1 ± 0.3 (31.7 ± 2.6)		
Cholesterol (mmol/l)	<5.0	4.2 ± 0.7			4.7 ± 1.2		
HDL (mmol/l)	>1.0	1.5 ± 0.4			1.2 ± 0.2 #		
LDL (mmol/l)	<3.0	2.3 ± 0.7			3.1 ± 1.0		
TSH (mU/l)	(0.3 - 4.2)	1.8 ± 0.8	1.6 ± 0.9	1.4 ± 0.7	1.8 ± 0.4	1.5 ± 0.6	1.2 ± 0.5**
T3v (pmol/l)	(3.1 - 6.8)	4.8 ± 0.4	4.9 ± 0.6	5.2 ± 0.6	5.4 ± 0.6 #	5.2 ± 0.8	5.1 ± 0.7
T4v (pmol/l)	(11 - 22)	16.1 ± 2.3	15.9 ± 2.3	16.4 ± 2.1*	15.2 ± 1.7	15.1 ± 1.8	15.6 ± 1.5
Triglycerides (mmol/l)	(0.45-2.6)	0.7 ± 0.2	0.7 ± 0.3	0.8 ± 0.3**	1.0 ± 0.6	1.0 ± 0.6	1.1 ± 0.6*
Free fatty acids (mmol/l)			0.4 ± 0.1	0.6 ± 0.1**		0.5 ± 0.2	0.5 ± 0.2
Lactate (mmol/l)	(0.6-2.4)		0.8 ± 0.1	1.1 ± 0.5*		0.9 ± 0.2	1.1 ± 0.5
Noradrenaline (nmol/l)	(0.59 - 3.55)		2.4 ± 1.0	6.4 ± 2.6***		2.6 ± 0.7	5.1 ± 1.9**
Energy expenditure (kcal/day)			1664 ± 195	1907 ± 293*		2107 ± 202	2305 ± 207*
Data are mean ± S.D. #P<0.05, ##P<0.01, Independent T-Test comparing screening values of lean and overweight subjects. *P<0.05, **P<0.01, ***P=0.001 Paired T-test comparing values within group before and after cold exposure.							

Figure Legends

Figure 1. A. Clincial PET study design. Each subject (lean n=9, overweight n=9) participated in imaging with [^{18}F]FMPEP-d_2 PET/CT in **B.** room temperature and **C.** cold conditions, and **D.** [^{18}F]FDG PET/MRI in cold conditions. Coronal PET images from one lean study subject, arrows depict supraclavicular BAT. **E.** Cold exposure increased BAT fractional uptake rate (FUR) of [^{18}F]FMPEP-d_2 in cold. Overweight (OW) subjects had a blunted cold response in BAT. **F.** BAT glucose uptake correlated with BAT [^{18}F]FMPEP-d_2 FUR in cold conditions. **G.** Image-guided human BAT biopsies (lean n=5, overweight n=4) confirmed cannabinoid receptor (CB) mRNA expression in BAT. CB1 mRNA expression was higher than CB2 mRNA expression. **H-I.** β3-adrenoreceptor and UCP1 mRNA expression in human BAT. **J.** Pearson's correlation between UCP1 mRNA expression in BAT and [^{18}F]FMPEP-d_2 FUR in BAT (n=9) and **K.** glucose uptake in BAT (n=8). Data pooled from lean (white triangle) and overweight (black circle) subjects. *P<0.05, **P<0.01.

Figure 2. A. [^{18}F]FMPEP-d_2 uptake at baseline conditions and during cold exposure of lean and overweight subjects in BAT, subcutaneous white adipose tissue (SC WAT), intraperitoneal white adipose tissue (IP WAT), muscle and brain gray matter. *Indicates paired t-test between baseline and cold conditions *P<0.05, **P<0.01, (*)P=0.07. ¤ Indicates independent t-test between lean and overweight groups ¤P<0.05, ¤¤P<0.01. **B.** Pearson's correlation between BMI and [^{18}F]FMPEP-d_2 uptake in cold of lean (triangle) and overweight (circle) subjects. **C.** PET brain images depicting fractional uptake rate (FUR) of [^{18}F]FMPEP-d_2 of one lean and one overweight subject at baseline and cold conditions. **D-E.** Pearson's correlation between [^{18}F]FMPEP-d_2 FUR values of BAT and the midbrain region of interest in cold and baseline conditions, pooled lean and overweight subjects.

Figure 3.A-D. Pharmacological intervention in rodent BAT. **A.** Dynamic uptake of [^{18}F]FMPEP-d_2 into BAT over time. **B.** Volume distribution (V_T) values of [^{18}F]FMPEP-d_2 uptake and retention in BAT calculated from dynamic PET data, with image-derived arterial, metabolite corrected input. **C.** Effect on glucose uptake into BAT. **D.** Modulation of perfusion based on the [^{18}F]FDG extraction parameter K1, derived from kinetic modeling of [^{18}F]FDG PET data. β3-AR agonist CL 316243 (blue), CB1-receptor antagonist rimonabant (red), basal physiology (black). **E.** mRNA expression of CB1 and CB2 receptors in human brown adipocytes (BA) and **F.** white adipocytes (WA). Noradrenaline (NA; 1 µM) stimulation for 16 h increases CB1 mRNA expression in BA but not in WA. Cannabinoid type 1 receptor (CB1), cannabinoid type 2 receptor (CB2). **G.** Glucose uptake and **H.** glycerol release in a human brown adipocyte cell line (hMADS) during pharmacological intervention with CB1 receptor antagonist, CB1 receptor agonist, CB2 receptor antagonist and CB2 receptor agonist, combined with noradrenaline (NA; 1 µM). *P<0.05, **P<0.01, ***P<0.001, ****P<0.0001. NS = non-significant.

Figure 1.

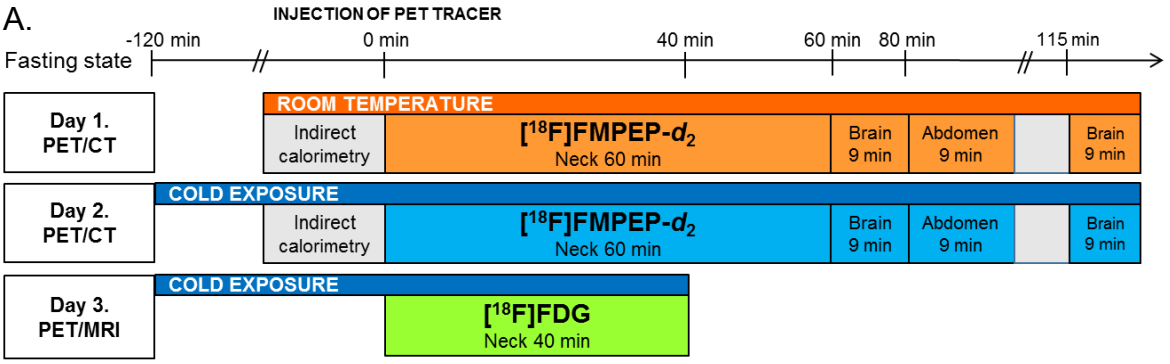
A.
INJECTION OF PET TRACER
-120 min
0 min
40 min
60 min
80 min
115 min
Fasting state
Day 1. PET/CT
ROOM TEMPERATURE
Indirect calorimetry
[18F]FMPEP-d2 Neck 60 min
Brain 9 min
Abdomen 9 min
Brain 9 min
Day 2. PET/CT
COLD EXPOSURE
Indirect calorimetry
[18F]FMPEP-d2 Neck 60 min
Brain 9 min
Abdomen 9 min
Brain 9 min
Day 3. PET/MRI
COLD EXPOSURE
[18F]FDG Neck 40 min

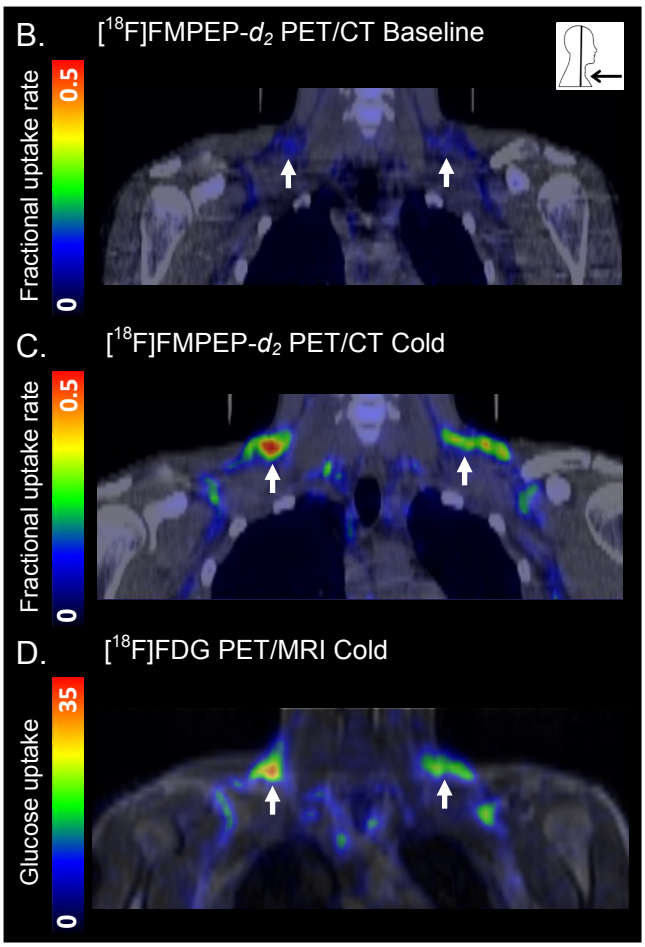
B.
[18F]FMPEP-d2 PET/CT Baseline
Fractional uptake rate
0.5
0
C.
[18F]FMPEP-d2 PET/CT Cold
Fractional uptake rate
0.5
0
D.
[18F]FDG PET/MRI Cold
Glucose uptake
35
0

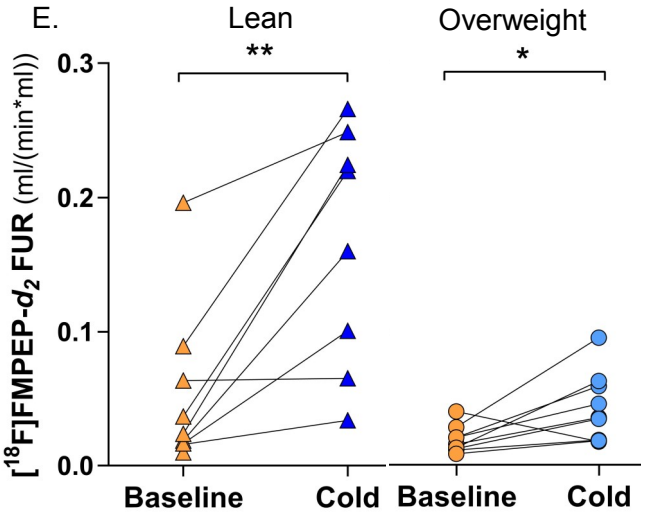
E.
Lean
Overweight
**
*
[18F]FMPEP-d2 FUR (ml/(min*ml))
0.3
0.2
0.1
0.0
Baseline
Cold
Baseline
Cold

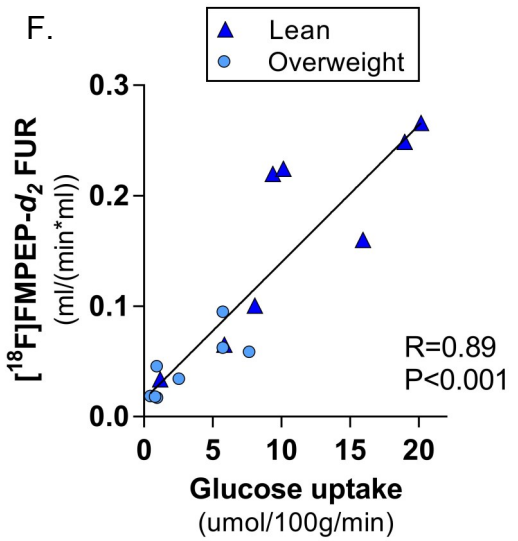
F.
Lean
Overweight
[18F]FMPEP-d2 FUR (ml/(min*ml))
0.3
0.2
0.1
0.0
R=0.89
P<0.001
0
5
10
15
20
Glucose uptake
(umol/100g/min)

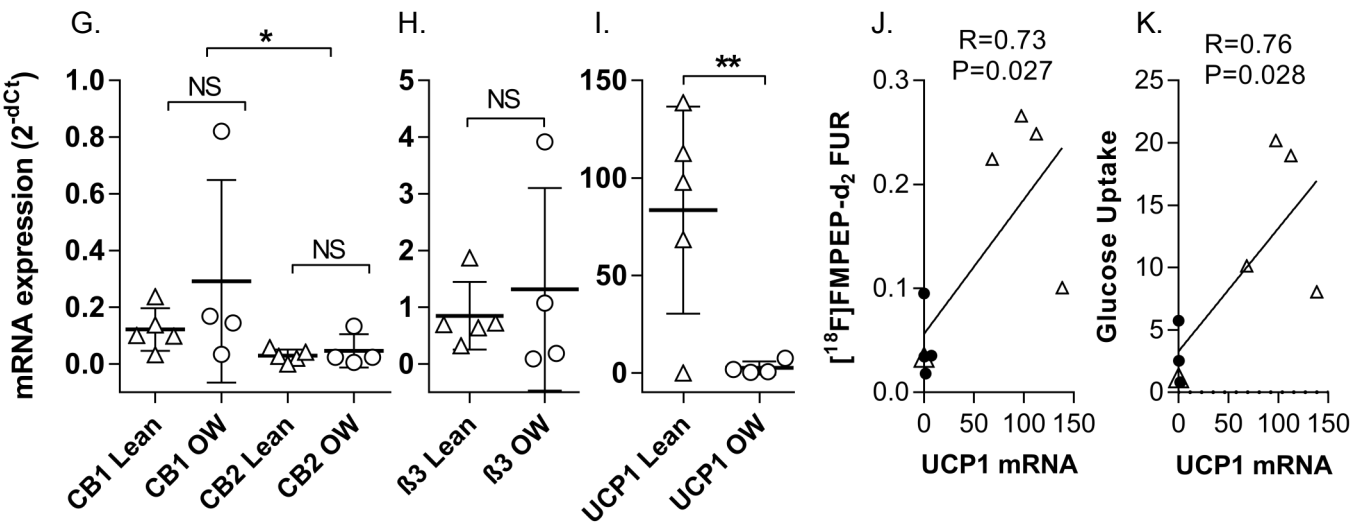
G.
*
NS
NS
mRNA expression (2-dCt)
1.0
0.8
0.6
0.4
0.2
0.0
CB1 Lean
CB1 OW
CB2 Lean
CB2 OW
H.
NS
5
4
3
2
1
0
ß3 Lean
ß3 OW
I.
**
150
100
50
0
UCP1 Lean
UCP1 OW
J.
R=0.73
P=0.027
[18F]FMPEP-d2 FUR
0.3
0.2
0.1
0.0
0
50
100
150
UCP1 mRNA
K.
R=0.76
P=0.028
Glucose Uptake
25
20
15
10
5
0
0
50
100
150
UCP1 mRNA

Figure 2.

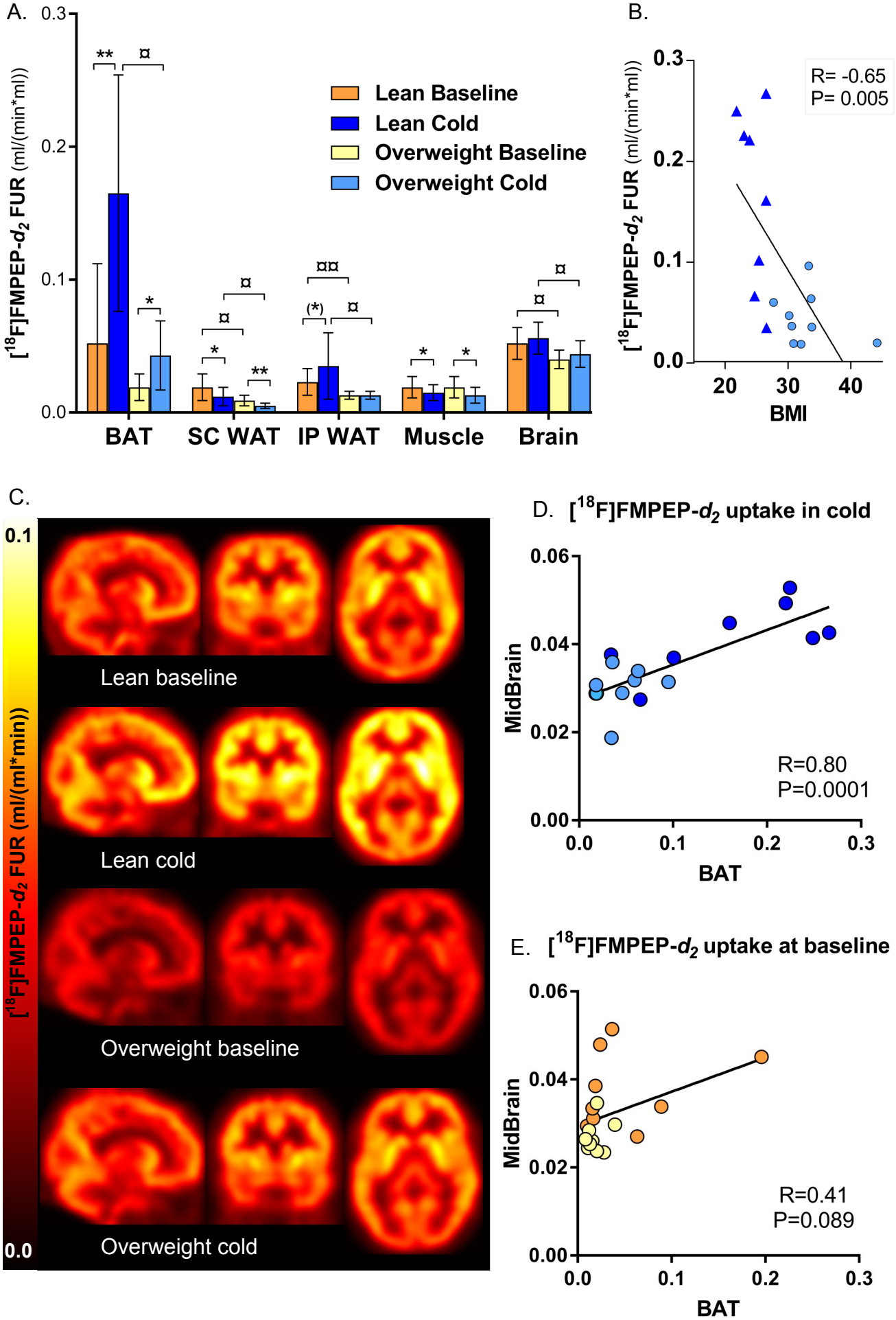
A.
[18F]FMPEP-d2 FUR (ml/(min*ml))
0.3
0.2
0.1
0.0
Lean Baseline
Lean Cold
Overweight Baseline
Overweight Cold
BAT
SC WAT
IP WAT
Muscle
Brain
B.
[18F]FMPEP-d2 FUR (ml/(min*ml))
R= -0.65
P= 0.005
BMI
C.
[18F]FMPEP-d2 FUR (ml/(ml*min))
0.1
0.0
Lean baseline
Lean cold
Overweight baseline
Overweight cold
D. [18F]FMPEP-d2 uptake in cold
MidBrain
BAT
R=0.80
P=0.0001
E. [18F]FMPEP-d2 uptake at baseline
MidBrain
BAT
R=0.41
P=0.089

Figure 3.

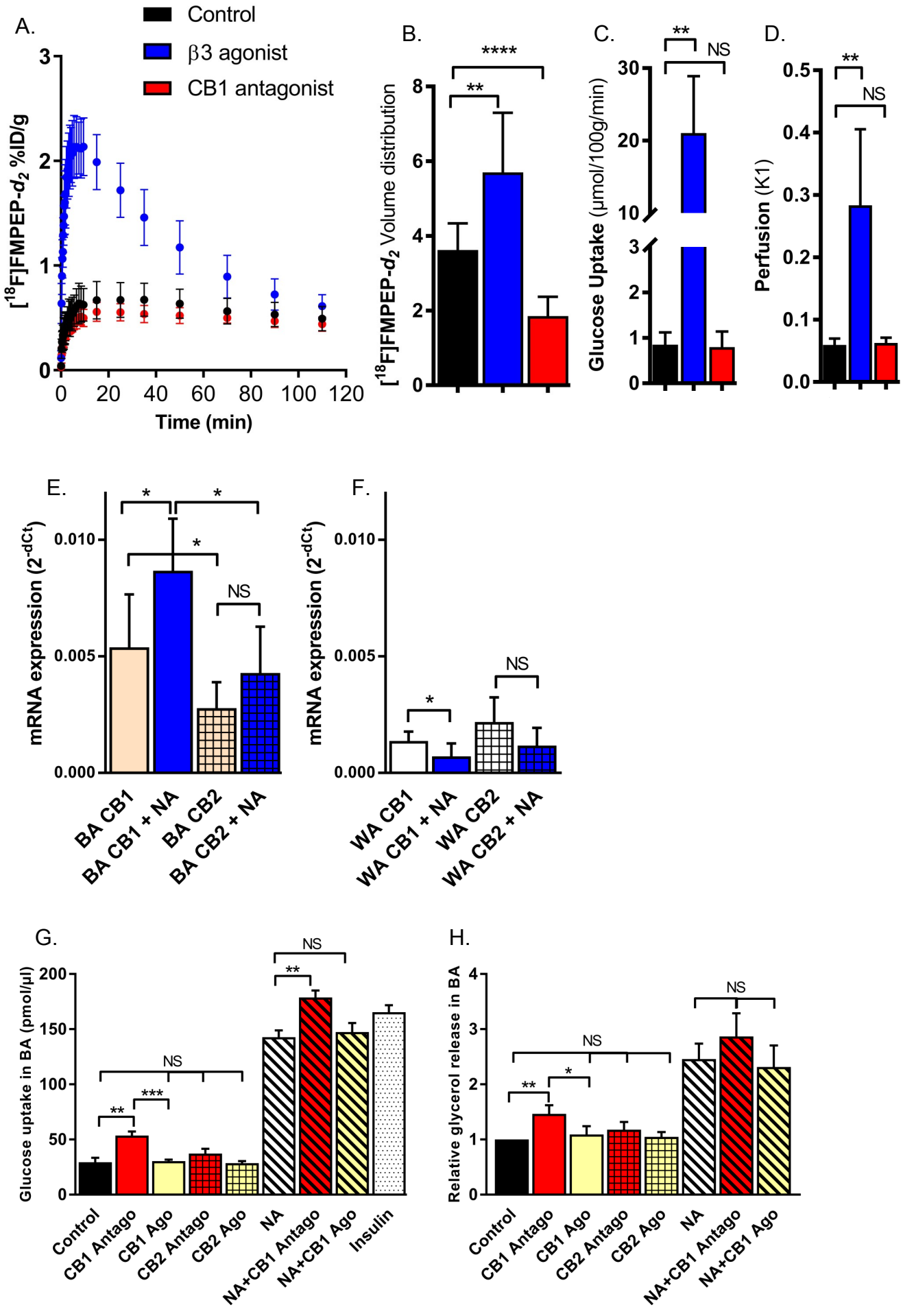
A.
Control
β3 agonist
CB1 antagonist
[18F]FMPEP-d2 %ID/g
Time (min)
B.
[18F]FMPEP-d2 Volume distribution
C.
Glucose Uptake (µmol/100g/min)
NS
D.
Perfusion (K1)
NS
E.
mRNA expression (2-dCt)
BA CB1
BA CB1 + NA
BA CB2
BA CB2 + NA
F.
mRNA expression (2-dCt)
WA CB1
WA CB1 + NA
WA CB2
WA CB2 + NA
G.
Glucose uptake in BA (pmol/µl)
Control
CB1 Antago
CB1 Ago
CB2 Antago
CB2 Ago
NA
NA+CB1 Antago
NA+CB1 Ago
Insulin
H.
Relative glycerol release in BA
Control
CB1 Antago
CB1 Ago
CB2 Antago
CB2 Ago
NA
NA+CB1 Antago
NA+CB1 Ago